



Universidad Autónoma  
de Madrid

**Biblos-e Archivo**  
Repositorio Institucional UAM

Repositorio Institucional de la Universidad Autónoma de Madrid  
<https://repositorio.uam.es>

Esta es la **versión de autor** del artículo publicado en:  
This is an **author produced version** of a paper published in:

Sensors and Actuators B: Chemical 274 (2018): 310-317

DOI: <https://doi.org/10.1016/j.snb.2018.07.124>

**Copyright:** © 2018 Elsevier Ltd. This manuscript version is made available under the CC-BY-NC-ND 4.0 license <http://creativecommons.org/licenses/by-nc-nd/4.0/>

El acceso a la versión del editor puede requerir la suscripción del recurso  
Access to the published version may require subscription

1     **MoS<sub>2</sub> nanosheets for improving analytical performance of lactate biosensors**

2  
3     Ana María Parra-Alfambra<sup>a</sup>, Elena Casero<sup>a</sup>, Luis Vázquez<sup>b</sup>, Carmen Quintana<sup>a</sup>,  
4     María del Pozo<sup>a</sup>, María Dolores Petit-Domínguez<sup>a\*</sup>

5  
6  
7     <sup>a</sup>*Departamento de Química Analítica y Análisis Instrumental. Facultad de Ciencias.*  
8     *c/ Francisco Tomás y Valiente, N°7. Campus de Excelencia de la Universidad*  
9     *Autónoma de Madrid. 28049 Madrid. Spain*  
10    <sup>b</sup>*ESISNA group, Materials Science Factory, Instituto de Ciencia de Materiales de*  
11    *Madrid (CSIC). c/ Sor Juana Inés de la Cruz, N°3. Campus de Excelencia de la*  
12    *Universidad Autónoma de Madrid. 28049 Madrid. Spain*

13  
14    \* Corresponding author: [mdolores.petit@uam.es](mailto:mdolores.petit@uam.es)

## Abstract

In this paper, a new 2D lactate electrochemical biosensor was developed. It was based on the incorporation of molybdenum disulfide ( $\text{MoS}_2$ ) platelets, obtained by an exfoliation method, onto the surface of a glassy carbon (GC) electrode, together with lactate oxidase enzyme (LOx). For the sensor construction, conditions regarding the exfoliation solvent type, as well as both the size and amount of  $\text{MoS}_2$ , were optimized. The biosensor platform (GC/ $\text{MoS}_2$ /LOx) was topographically characterized by atomic force microscopy (AFM) and the charge transfer process occurring at the electrode interface was studied by electrochemical impedance spectroscopy (EIS). The GC/ $\text{MoS}_2$ /LOx biosensor was applied to the determination of lactate in presence of hydroxymethylferrocene (HMF) as a redox mediator. Electrocatalytic effect of the system  $\text{MoS}_2$ /LOx was evaluated by comparing the cyclic voltammetric biosensor response with those obtained for biosensors incorporating only one of the components ( $\text{MoS}_2$  or LOx) onto the electrode surface. Biosensors containing both components exhibit the best electrocatalytic response. From the calibration curve obtained at +0.30 V, the following analytical parameters were obtained: linear concentration range from 0.056 to 0.77 mM, high sensitivity ( $6.2 \mu\text{A mM}^{-1}$ ), good detection limit ( $17 \mu\text{M}$ ) and reproducibility ( $\text{RSD} = 4.7\%$ ).

**Keywords:** molybdenum disulfide, electrochemical biosensor, lactate oxidase, cyclic voltammetry, atomic force microscopy, electrochemical impedance spectroscopy.

## 1. Introduction

The employment of 2D nanomaterials, such as graphene, for the development of enzymatic based biosensors has attracted great attention during the last decade as a way to obtain devices with improved analytical performance [1–3]. The excellent graphene properties enable the implementation of the detection. In particular, graphene modified electrodes offer a high surface area to load a high amount of enzymes, increasing sensitivity. Moreover, in the case of electrochemical biosensors, the excellent graphene conductivity facilitates the redox transfer between the enzyme and the electrode surface [4,5]. In a natural further step, the incorporation of other recently discovered 2D materials into biosensing devices, such as the transition metal dichalcogenides (TMDs), is of potential interest [6,7,8]. TMDs are graphene analogues formed by stacking S-TM-S sheets through Van der Waals forces. As a result of the weak forces between layers, single or few layers of these materials can be easily exfoliated from the bulk by mechanical cleavage, sonication in common solvents or ion intercalation/sonication methods, among others [9,10]. Due to their interesting mechanical, electrical and optical properties, the resulting 2D materials nanosheets have been studied and profusely applied in catalysis, energy storage and electronics [11–15]. TMDs application to sensing purposes is a current trend that lies on the large surface area and fast electron transfer of these materials. However, compared with the above-mentioned applications, the employment of TMDs nanosheets in sensing devices is still scarce, being almost exclusively focused on molybdenum disulfide [16–19]. In this sense, several groups have constructed MoS<sub>2</sub> based electrochemical sensors for detecting compounds such as glucose [20–22], dopamine [23,24], eugenol [25], tryptophan [16,26] and bisphenol [27,28]. The good analytical properties obtained for these sensors evidence that the use of MoS<sub>2</sub> is a promising strategy for determining compounds of interest. In contrast, the

employment of TMDs for developing electrochemical enzymatic biosensors remains almost unexplored. Among the developed TMDs based electrochemical biosensing platforms, the majority involved the use of MoS<sub>2</sub> nanosheets and the enzyme glucose oxidase [29–31]. Beyond glucose oxidase, implemented MoS<sub>2</sub> based biosensors involving laccase [32] and horseradish peroxidase [33] have been also reported, allowing the determination of caffeic acid and hydrogen peroxide, respectively. Recently, Pumera et al. have demonstrated that the employment of TMDs in enzymatic biosensors for electrochemical detection of the pesticide fenitrothion, via an inhibition pathway, offers enhanced responses in comparison with biosensors without TMDs [34]. The satisfactory analytical properties obtained in the above-mentioned studies indicate that TMDs, particularly MoS<sub>2</sub>, present good biocompatibility allowing also a high enzyme loading. Therefore, they are promising candidates for biosensing.

In the present work, we study the effect of incorporating MoS<sub>2</sub> into biosensing platforms for lactate determination. The development of implemented biosensors for the determination of lactate is of great interest in several fields such as clinical diagnostics, food industry and fermentation processes. In the literature, we can find electrochemical lactate enzymatic biosensors based on the employment of nanomaterials with different dimensionality, such as metal nanoparticles [35–37], diamond nanoparticles [38–40], graphene oxide [41], reduced graphene [42–45] or carbon nanotubes [46–48]. However, as far as we know, there are no biosensors for lactate determination that include only TMDs and lactate oxidase. In order to develop the biosensing platform, we have obtained MoS<sub>2</sub> sheets by exfoliation in different solvents and we have deposited them, together with lactate oxidase, on a glassy carbon (GC) electrode surface. Once the optimum conditions regarding the exfoliation solvent and both the size and amount of MoS<sub>2</sub> were established, the topographical surface of the MoS<sub>2</sub>/GC was imaged by

atomic force microscopy (AFM). The biosensor was employed for lactate determination in order to prove that MoS<sub>2</sub> offers a good platform for lactate oxidase accommodation leading to an enhancement of the biosensing performance.

## **2. Experimental Section**

### **2.1. Materials**

Molybdenum disulfide (99%, 2 μm and 90 nm in size), Lactate oxidase (LOx, EC 232-841-6 from *Pediococcus* species) lyophilized powder containing 41 units / mg solid, L-(+)-lactic acid lithium salt 97%, dopamine, hydroxymethyl-ferrocene (HMF), N-methyl pyrrolidone (NMP), dimethylformamide (DMF), ethanol (EtOH), isopropyl alcohol (IPA), potassium ferrocyanide, potassium ferricyanide, ascorbic acid, uric acid and citric acid were purchased from Sigma Aldrich ([www.sigmaaldrich.com](http://www.sigmaaldrich.com)). Lactate oxidase stock solutions were prepared dissolving 1.3 mg of the LOx lyophilized powder in 250 μL of 0.1M phosphate buffer solution (pH = 7.0), aliquoted (10 μL) and stored at -30°C. Under these conditions, the enzymatic activity remains stable for several weeks. Buffer solutions were prepared using sodium phosphate from Merck ([www.merck.com](http://www.merck.com)). All solutions were prepared just prior to use with purified water obtained from a Millipore Milli-Q-System ([www.millipore.com](http://www.millipore.com)).

### **2.2. Experimental techniques**

Cyclic voltammetry (CV) and electrochemical impedance spectroscopy (EIS) studies were performed with an Ecochemie Autolab PGSTAT302 N system (Utrecht, The Netherlands, [www.ecochemie.nl](http://www.ecochemie.nl)). The electrochemical cell consisted of an Ag/AgCl (Metrohm, 3.0 M KCl) reference electrode, a platinum auxiliary electrode and a bare or modified glassy carbon working electrode (3 mm internal diameter). Cyclic voltammetry was carried out using the biosensors in the presence of HMF (which acts

as soluble mediator in solution) and in the presence or absence of L-lactate. Solutions were deaerated with nitrogen gas before use, and the gas flow was kept over the solutions during experiments.

EIS experiments were performed in a 0.1 M phosphate buffer solution (pH = 7), containing 10 mM  $\text{K}_3\text{Fe}(\text{CN})_6$  /  $\text{K}_4\text{Fe}(\text{CN})_6$ . A sinusoidal potential modulation of  $\pm 10$  mV amplitude in the  $10^5$  Hz- $10^{-2}$  Hz frequency range, spaced logarithmically (120 per 8 decades), was superimposed onto the formal potential of the redox couple,  $[\text{Fe}(\text{CN})_6]^{3-/4-}$ .

Atomic force microscopy (AFM) studies were carried out using two different systems, a Nanoscope IIIa (Veeco) equipment and an Agilent 5500 Picoplus. Both systems were employed for topographical analysis, while the last one was used for single-pass Kelvin Force Microscopy (KFM) imaging. For morphological studies, silicon cantilevers with nominal force constant of 40 N/m and radius of curvature of 8 nm were employed and the dynamic mode was employed (Blucker). The KFM data were obtained with ANSCM-PT cantilevers (from AppNano), which have a force constant in the 1-5 N/m range and nominal radius of curvature less than 30 nm. In the KFM measurements, the sample was grounded. KFM measures the Contact Potential Difference (CPD), which is the difference between the work function values of the imaged sample location and that of the tip. The images taken with the Veeco equipment had 512 x 512 pixels whereas those obtained with Picoplus had 1024 x 1024 or 4096 x 4096 pixels.

## **2.3. Procedures**

### ***2.3.1. Synthesis of $\text{MoS}_2$ platelets***

$\text{MoS}_2$  atomic layers were synthesized from  $\text{MoS}_2$  nano-sized as starting materials through liquid exfoliation, following adapted published procedures [49–51]. We have employed four different solvents such as NMP, DMF, EtOH/water and IPA/water. The

last two mixtures in a 45:55 v/v ratio. Briefly, 25, 50, 75 or 100 mg of the commercial MoS<sub>2</sub> powder (90 nm or 2 µm in size) were mixed under sonication for 2 hours with 10.0 mL of the corresponding solvent. Since several authors [49-51] have demonstrated that sophisticated ultrasonic equipment to obtain MoS<sub>2</sub> sheets with a high dispersion degree are not necessary, the sonication procedure was carried out using a JP Selecta ultrasonic bath sonicator at nominal power output of 100 W. After sonication, dispersions were maintained 24 hours at 4°C and then centrifuged at 1500 rpm during 45 minutes. The supernatant was collected for its use in the GC electrode surface modification.

### **2.3.2. Preparation of the electrochemical sensors**

Glassy carbon electrode surfaces were polished with 1 µm diamond paste (Buehler) and rinsed with water. GC electrodes were then modified by placing 10 µL of MoS<sub>2</sub> exfoliated in NMP, DMF, EtOH/water or IPA/water solvent, leaving air-dry and finally 5 µL of the LOx stock solution were dropped on this surface and left to dry.

Sensors containing only MoS<sub>2</sub> or LOx were obtained by modifying the GC electrode with 10 or 5 µL respectively of the corresponding solution and leaving air-dry it.

### **2.3.3. Evaluation of the electrochemical sensors**

Evaluation of all electrochemical sensors were carried out by substituting the natural electron acceptor (O<sub>2</sub>) by an artificial mediator (hydroxymethylferrocene, HMF), in the following reaction catalysed by the enzyme LOx: Lactate + O<sub>2</sub> → Pyruvate + H<sub>2</sub>O<sub>2</sub>. This strategy allows following the electrochemical behaviour of HMF at +0.30 V, instead of detecting the generated hydrogen peroxide. Consequently, the contribution of interfering substances, which could be oxidized at the high potential required for H<sub>2</sub>O<sub>2</sub> detection, are minimized.



As can be observed in scheme 1, the enzyme catalyzes the oxidation of lactate to pyruvate, while the electrons involved in the process are immediately transferred to the oxidized form of the soluble redox mediator (HMF), regenerating the enzyme activity. The re-oxidation of HMF on the electrode surface leads to a bioelectrocatalytic response that can be observed, which is proportional to the amount of lactate present in the solution. Therefore, in the absence of lactic acid, the typical redox response of the ferrocene/ferrocinium process at +0.30 V in aqueous media is expected. The addition of lactic acid will lead to an enhancement of the anodic peak current concomitant with a decrease of the cathodic peak current as long as the sensor components give rise to an electrocatalytic effect.

#### ***2.3.4. Preparation of the samples for AFM measurements***

Samples for AFM measurements were prepared by placing 10  $\mu\text{L}$  of  $\text{MoS}_2$  exfoliated in NMP onto Si surfaces, left to dry and finally 5  $\mu\text{L}$  of the LOx stock solution were dropped on it. Sensors containing only  $\text{MoS}_2$  were obtained by modifying the Si surface with 10  $\mu\text{L}$  of  $\text{MoS}_2$  exfoliated in NMP. Likewise, additional samples were prepared by depositing a drop of the solvent NMP (10  $\mu\text{L}$ ) in a flat silicon surface and let dry. In the AFM experiments, samples containing 2  $\mu\text{m}$   $\text{MoS}_2$  particles were analysed.

### **3. Results and discussion**

#### **3.1. Parameters optimization for biosensor construction**

##### ***3.1.1. Exfoliation of $\text{MoS}_2$ in different solvents.***

According to Coleman et al. [49-51] in order to produce stable  $\text{MoS}_2$  sheet dispersions through sonication in a liquid medium, it is convenient to use solvents with surface energies similar to those of the material to be exfoliated. Taking into account both that the surface energy of  $\text{MoS}_2$  is about 70  $\text{mJ m}^{-2}$  and that the liquid surface

energy values of the solvents are around  $30 \text{ mJ m}^{-2}$  above their surface tensions, we have selected the following four solvents: NMP, DMF, IPA/water and EtOH/water. These solvents have the following surface tensions:  $40.7 \text{ mN m}^{-1}$  (NMP),  $34.4 \text{ mN m}^{-1}$  (DMF),  $22.3 \text{ mN m}^{-1}$  (EtOH),  $20.8 \text{ mN m}^{-1}$  (IPA) and  $72.8 \text{ mN m}^{-1}$  ( $\text{H}_2\text{O}$ ) (the units  $\text{mN m}^{-1}$  and  $\text{mJ m}^{-2}$  are equivalent). In order to evaluate them, samples containing 75 mg of molybdenum disulfide were exfoliated in 10.0 mL of the solvent tested. Afterwards, cyclic voltammograms of four modified electrodes, prepared with  $\text{MoS}_2$  exfoliated in the different solvents and LOx (GC/ $\text{MoS}_2$ /LOx), were recorded in a 0.1 M pH = 7.0 phosphate buffer containing 1.0 mM HMF. A typical cyclic voltammogram is shown in Figure 1, curve a, for the ferrocene/ferrocinium process at GC/ $\text{MoS}_2$ /LOx modified electrode with a formal potential of +0.30 V. Similar voltammograms are obtained for all the solvents tested in absence of lactate (here it is only shown that obtained using NMP to exfoliate the  $\text{MoS}_2$ ). In presence of 0.65 mM L-lactate (Figure 1, curves b-e), for the different solvents employed: IPA/water (b), EtOH/water (c), DMF (d) and NMP (e), it is observed both an enhancement of the anodic peak current and a decrease of the cathodic peak current, which is consistent with a clear electrocatalytic effect. However, this enhancement is higher when NMP is used as solvent (curve e), with a threefold increase in the anodic peak current with respect to curve a. Results confirm that the solvent selection is fundamental for obtaining adequate  $\text{MoS}_2$  sheet dispersions and, in this sense, the most suitable solvent is NMP with a surface energy about  $70.7 \text{ mJ m}^{-2}$ , which is the most similar to the  $\text{MoS}_2$  surface energy ( $70 \text{ mJ m}^{-2}$ ). Consequently, NMP was selected as the most adequate exfoliating solvent to obtain  $\text{MoS}_2$  sheet dispersions.

### ***3.1.2. Selection of the $\text{MoS}_2$ powder particle size.***

Once the exfoliating solvent to obtain  $\text{MoS}_2$  sheet dispersions was chosen, two different  $\text{MoS}_2$  powder particle sizes, 90 nm and 2  $\mu\text{m}$ , were compared in order to

obtain the most suitable sensor. Figure 2 shows voltammograms obtained for two different GC electrodes modified with LOx and MoS<sub>2</sub> of 2  $\mu$ m (curve b) or 90 nm (curve c) in NMP in the presence of lactate. Similar voltammograms are obtained for the two sizes tested in absence of lactate (here it is shown that obtained using 90 nm MoS<sub>2</sub> powder nanoparticle size, curve a). In presence of lactate, it is clearly observed, in both cases, an increase of the anodic peak current with respect to this current in absence of lactate (curve a) with an increase of about 2.3 and 3 times for 2  $\mu$ m and 90 nm, respectively. The fact that the 90 nm MoS<sub>2</sub> based biosensor leads to a different response than the 2  $\mu$ m MoS<sub>2</sub> one is not surprising, since according to some authors, interaction between nanoparticles and biological material are influenced by the nanomaterial particle size [52]. It is worth noting that in the mild sonication conditions used, it will be easier to obtain more adequate dispersions from a smaller particle size. Therefore, 90 nm MoS<sub>2</sub> was chosen as nanoparticle size for the following studies.

### ***3.1.3. Selection of the concentration of MoS<sub>2</sub> dispersions.***

It was also expected that the MoS<sub>2</sub>/LOx amount ratio in the modified electrode surfaces could affect the enhancement of the anodic peak current due to the electrocatalytic effect. In this sense, different amounts of 90 nm MoS<sub>2</sub> were exfoliated with 10.0 mL of NMP, as it is explained in the *Procedures* section, and the resulting dispersions used to modify the GC electrode surface together with a fixed amount of enzyme. Intensities of the anodic peak current of modified GC electrodes measured at +0.30 V are shown in Figure 3.

From this figure, it can be seen that as the concentration of MoS<sub>2</sub> increases, the peak current intensity also increases up to a value of MoS<sub>2</sub> concentration of 7.5 mg mL<sup>-1</sup>, from which the peak current intensity decreases slightly. Accordingly, this concentration is chosen for the preparation of the modified electrodes. A reason for this

behavior could be that the increase of MoS<sub>2</sub> amount leads to an increase in the specific surface area and therefore in the loaded enzyme amount. However, up to a certain concentration value, in our case around 7.5 mg mL<sup>-1</sup>, the great amount of MoS<sub>2</sub> makes more difficult the electron transfer on the electrode surface.

### **3.2. Morphological characterization: AFM measurements**

In order to address the morphological study of the MoS<sub>2</sub> surfaces, a first step consisted in analyzing the features, if any, associated just to the solvent employed for MoS<sub>2</sub> exfoliation. For this purpose, we deposited a drop of the solvent in a flat silicon surface and let it dry. This surface was imaged and a characteristic image is shown in Figure 4a. Clearly, many morphological features are due to the solvent. The most usual ones are the rounded structures that appear scattered on the surface, particularly at the middle right part of the image, that have an average size of 170 nm and heights in the 10-15 nm range. In addition, brighter and wider spots are also found, as those two at the top part of the image as well as those found at the bottom part, with sizes close to 500 nm and heights larger than 50 nm. Finally, large corrugated aggregates as large as 7 microns and with heights in the 70-100 nm range are also imaged as that located at the top left part of the figure.

This rich morphology due just to the solvent employed poses a problem when trying to image the MoS<sub>2</sub> flakes prepared with this solvent in the surfaces. A good criterion to locate the MoS<sub>2</sub> structures consists in searching for plateau-like, 2D, structures and heights in the nanometer range, such as those shown in Figure 4b. In this figure up to seven such 2D structures are located. The surface profile along three of them (solid line) is shown in Figure 4c. From these data we can assess that their height is close to 1 nm and the lateral size between 300 and 600 nm.

Furthermore, in order to show that the imaged flakes are different from the rounded structures coming from the solvent, we have performed KFM measurements with the goal to detect a different contrast in the contact potential difference (CPD) in both regions. With this purpose, we have chosen to image a larger 2D flake because of the relatively large radius of the KFM tip. Thus, Figures 4d and 4e show a topographical image of a flake and its corresponding KFM image, respectively. Clearly, the CPD contrast is smaller at the flake than at the rounded structure due to the solvent. This fact then confirms that the flakes are not structures associated to the solvent.

Finally, we have also imaged by AFM under ambient conditions the sample containing both MoS<sub>2</sub> exfoliated in NMP and LOx (Figures 4 f-h). First, in Figure 4f is shown a large MoS<sub>2</sub> flake, with a height close to 2 nm, in whose top surface are found globular structures with lateral sizes in the 15 nm range and heights close to 3 nm as shown in Figure 4g. Taking into account that the tip convolution effects increases the lateral size and the tip load deforms vertically the soft structure, these dimensions are compatible with those of the LOx. Figure 4h corresponds to other sample in which now the MoS<sub>2</sub> flakes are smaller with heights close to 3 nm. Similar globular structures are found on the plateaus and in many cases practically cover the whole flake.

### **3.3. Electrochemical impedance spectroscopy (EIS) studies**

EIS measurements have been performed in order to study the charge transfer process occurring at the electrode interface. Figure 5 shows Nyquist diagrams for GC, GC/MoS<sub>2</sub>, GC/LOx and GC/MoS<sub>2</sub>/LOx systems. Semicircles correspond to the charge transfer resistance limiting process ( $R_{CT}$ ) that is associated with the surface/electrolyte interface. The linear part corresponds to the diffusion-controlled process. The electron-transfer resistance ( $R_{CT}$ ) obtained from these Nyquist plots for a bare GC electrode was

565  $\Omega$ . When the electrode is modified only with LOx or MoS<sub>2</sub>, this value increases dramatically, reaching 78,560  $\Omega$  and 154,000  $\Omega$ , respectively. For both cases, the electron transfer between the redox probe, [Fe(CN)<sub>6</sub>]<sup>3-/4-</sup> and the glassy carbon electrode surface is hampered, particularly for the GC/MoS<sub>2</sub> system. However, when the GC electrode is modified simultaneously with MoS<sub>2</sub> and LOx, an intermediate R<sub>CT</sub> value is obtained (112,000  $\Omega$ ), demonstrating that the presence of the enzyme diminishes the high electron transfer resistance provided by MoS<sub>2</sub>. This behaviour has been previously observed in other enzymatic biosensing systems [53-55].

#### **3.4. Response of the GC/MoS<sub>2</sub>/LOx sensor towards increasing L-lactate concentrations**

Figure 6 shows the cyclic voltammograms of GC/MoS<sub>2</sub>/LOx obtained for 1 mM HMF in the presence of increasing lactate concentrations (A) and the corresponding calibration curve (B) obtained from measurements of the current intensity at +0.30 V. The analytical properties, linear response, sensitivity as well as detection and quantification limits of the biosensor are obtained from the linear part of this calibration curve. As it can be seen, the calibration plot is linear over a concentration range from 0.056 to 0.77 mM, according to the following equation  $I (\mu A) = 0.19 (\pm 0.05) + 6.2 (\pm 0.1) C (mM)$ , with a correlation coefficient of 0.996. The sensitivity, calculated as the slope of the calibration curve, is 6.2  $\mu A mM^{-1}$ . The detection and quantification limits, obtained as the ratio between three and ten times the standard deviation of the blank signal and the sensitivity, are 17  $\mu M$  and 56  $\mu M$ , respectively.

The reproducibility was evaluated from the relative standard deviation (R.S.D. %) for four different biosensors at 0.25 mM lactate concentration level, obtaining a value of 4.7%.

According to previous studies [41, 43], the presence of just LOx on the GC electrode surface leads to a slight increment of the electrochemical analytical signal of 1 mM HMF in presence of L-lactate with respect to the same electrode in absence of L-lactate. Moreover, the response of bare GC and GC/MoS<sub>2</sub> electrodes are similar (data not shown). As expected, due to the absence of the enzyme, none of them do show any catalytic effect in presence of L-lactate. In contrast, the response of GC/MoS<sub>2</sub>/LOx is clearly better, which confirms that the combined presence of MoS<sub>2</sub> and LOx leads to an improved response. A possible explanation can be that the presence of MoS<sub>2</sub> induces a different positioning of the enzyme onto the electrode surface compared with that adopted on bare GC surface, leading to a conformational stabilization of the enzyme in a more adequate microenvironment and therefore to a higher functionality of the enzyme.

Table 1 shows the analytical properties of several lactate biosensors found in the literature [35–48]. As it can be observed, the developed biosensor shows similar analytical properties than those obtained for other biosensors also based in nanomaterials. However, it is worth noting that, as far as we know, there are not similar works in the literature that include only MoS<sub>2</sub> and the enzyme LOx together for lactate determination. From this point of view, this work demonstrates for the first time the synergistic effect of MoS<sub>2</sub> nanosheets and lactate oxidase in biosensing. Moreover, our simple biosensor design just requires the inclusion of MoS<sub>2</sub> as nanomaterial while most of the biosensors displayed in the table require a combination of different nanomaterials in their design.

In order to evaluate the applicability of the biosensor, we have studied dopamine, ascorbic acid, uric acid and citric acid as potential interferents. Results, displayed in table 2, show an increase of the analytical signal about 10% for a ratio [interferent]/[lactate] of 0.25, 0.53, 1 and 3, respectively.

#### 4. Conclusions

We have developed an electrochemical biosensor based on the incorporation of MoS<sub>2</sub> platelets, obtained by an exfoliation method, onto the surface of a glassy carbon electrode, together with lactate oxidase enzyme. The best biosensor response is obtained using NMP as exfoliation solvent and 7.5 mg mL<sup>-1</sup> of MoS<sub>2</sub> with a particle size of 90 nm. AFM images show that MoS<sub>2</sub> structures consist in 2D structures with lateral sizes between 300 and 600 nm and heights close to 1 nm. EIS studies show that when the electrode is modified only with MoS<sub>2</sub>, the electron transfer resistance value increases dramatically. In contrast, the combined presence of MoS<sub>2</sub> and LOx in the biosensor platform diminishes this high electron transfer resistance and leads to an enhanced electrocatalytic response towards increasing lactate concentrations. Good analytical parameters such as linear concentration range, sensitivity, detection and quantification limits are obtained in a simpler biosensor construction than many similar biosensors based on nanomaterials described in the literature.

#### 5. Acknowledgments

The authors would like to thank Ministerio de Economía, Industria y Competitividad (MAT2017-85089-C2-1-R, MAT2017-85089-C2-2-R) and the Comunidad Autónoma de Madrid (S2013/MIT-3029, NANOAVANSENS) for financial support.



## 359 6. References

- 360 [1] E.B. Bahadir, M.K. Sezgentürk, Applications of graphene in electrochemical  
361 sensing and biosensing, *TrAC - Trends Anal. Chem.* 76 (2016) 1–14.
- 362 [2] S. Kochmann, T. Hirsch, O.S. Wolfbeis, Graphenes in chemical sensors and  
363 biosensors, *TrAC - Trends Anal. Chem.* 39 (2012) 87–113.
- 364 [3] M. Pumera, Graphene in biosensing, *Mater. Today*. 14 (2011) 308–315.
- 365 [4] Y. Song, Y. Luo, C. Zhu, H. Li, D. Du, Y. Lin, Recent advances in  
366 electrochemical biosensors based on graphene two-dimensional nanomaterials,  
367 *Biosens. Bioelectron.* 76 (2016) 195–212.
- 368 [5] M. Pumera, A. Ambrosi, A. Bonanni, E.L.K. Chng, H.L. Poh, Graphene for  
369 electrochemical sensing and biosensing, *TrAC - Trends Anal. Chem.* 29 (2010)  
370 954–965.
- 371 [6] M. Pumera, A.H. Loo, Layered transition-metal dichalcogenides (MoS<sub>2</sub> and  
372 WS<sub>2</sub>) for sensing and biosensing, *TrAC - Trends Anal. Chem.* 61 (2014) 49–53.
- 373 [7] Y.-H. Wang, K.-J. Huang, X. Wu, Recent advances in transition-metal  
374 dichalcogenides based electrochemical biosensors: A review, *Biosens.*  
375 *Bioelectron.* 97 (2017) 305–316.
- 376 [8] R. Mas-Ballesté, C. Gómez-Navarro, J. Gómez-Herrero, F. Zamora, 2D  
377 materials: to graphene and beyond, *Nanoscale*. 3 (2011) 20–30.
- 378 [9] X. Huang, Z. Zeng, H. Zhang, Metal dichalcogenide nanosheets: preparation,  
379 properties and applications, *Chem. Soc. Rev.* 42 (2013) 1934.
- 380 [10] X. Li, J. Shan, W. Zhang, S. Su, L. Yuwen, L. Wang, Recent Advances in  
381 Synthesis and Biomedical Applications of Two-Dimensional Transition Metal  
382 Dichalcogenide Nanosheets, *Small*. 13 (2017) 1–28.
- 383 [11] M.A. Lukowski, A.S. Daniel, F. Meng, A. Forticaux, L. Li, S. Jin, Enhanced  
384 Hydrogen Evolution Catalysis from Enhanced Hydrogen Evolution Catalysis  
385 from Chemically Exfoliated Metallic MoS<sub>2</sub> Nanosheets, *J. Am. Chem. Soc.* 135  
386 (2013) 10274.
- 387 [12] D. Voiry, J. Yang, M. Chhowalla, Recent Strategies for Improving the Catalytic  
388 Activity of 2D TMD Nanosheets Toward the Hydrogen Evolution Reaction, *Adv.*  
389 *Mater.* (2016) 6197–6206.
- 390 [13] X. Wang, Q. Weng, Y. Yang, Y. Bando, D. Golberg, Hybrid two-dimensional  
391 materials in rechargeable battery applications and their microscopic mechanisms,  
392 *Chem. Soc. Rev.* 45 (2016) 4042–4073.
- 393 [14] B. Mendoza-Sánchez, Y. Gogotsi, Synthesis of Two-Dimensional Materials for  
394 Capacitive Energy Storage, *Adv. Mater.* (2016) 6104–6135.
- 395 [15] X. Song, Z. Guo, Q. Zhang, P. Zhou, W. Bao, D.W. Zhang, Progress of Large-  
396 Scale Synthesis and Electronic Device Application of Two-Dimensional  
397 Transition Metal Dichalcogenides, *Small*. 1700098 (2017) 1–22.
- 398 [16] K.J. Huang, L. Wang, J. Li, Y.M. Liu, Electrochemical sensing based on layered  
399 MoS<sub>2</sub>-graphene composites, *Sensors Actuators, B Chem.* 178 (2013) 671–677.
- 400 [17] K. Lee, R. Gatensby, N. McEvoy, T. Hallam, G.S. Duesberg, High-performance  
401 sensors based on molybdenum disulfide thin films, *Adv. Mater.* 25 (2013) 6699–  
402 6702.
- 403 [18] W. Zhang, P. Zhang, Z. Su, G. Wei, Synthesis and sensor applications of MoS<sub>2</sub> -  
404 based nanocomposites, *Nanoscale*. 7 (2015) 18364–18378.
- 405 [19] J. Ping, Z. Fan, M. Sindoro, Y. Ying, H. Zhang, Recent Advances in Sensing  
406 Applications of Two-Dimensional Transition Metal Dichalcogenide Nanosheets  
407 and Their Composites, *Adv. Funct. Mater.* 27 (2017) 1–18.

- [20] J. Huang, Y. He, J. Jin, Y. Li, Z. Dong, R. Li, *Electrochimica Acta* A novel glucose sensor based on MoS<sub>2</sub> nanosheet functionalized with Ni nanoparticles, *Electrochim. Acta.* 136 (2014) 41–46.
- [21] Y.J. Zhai, J.H. Li, X.Y. Chu, M.Z. Xu, F.J. Jin, X. Li, X. Fang, Z.P. Wei, X.H. Wang, MoS<sub>2</sub> microflowers based electrochemical sensing platform for non-enzymatic glucose detection, *J. Alloys Compd.* 672 (2016) 600–608.
- [22] X. Li, X. Du, Molybdenum disulfide nanosheets supported Au-Pd bimetallic nanoparticles for non-enzymatic electrochemical sensing of hydrogen peroxide and glucose, *Sensors Actuators, B Chem.* 239 (2017) 536–543.
- [23] V. Mani, M. Govindasamy, S.-M. Chen, R. Karthik, S.-T. Huang, Determination of dopamine using a glassy carbon electrode modified with a graphene and carbon nanotube hybrid decorated with molybdenum disulfide flowers, *Microchim. Acta.* 183 (2016) 2267–2275.
- [24] M. Cheng, X. Zhang, M. Wang, H. Huang, J. Ma, A facile electrochemical sensor based on well-dispersed graphene-molybdenum disulfide modified electrode for highly sensitive detection of dopamine, *J. Electroanal. Chem.* 786 (2017) 1–7.
- [25] Q. Feng, K. Duan, X. Ye, D. Lu, Y. Du, C. Wang, A novel way for detection of eugenol via poly (diallyldimethylammonium chloride) functionalized graphene-MoS<sub>2</sub> nano-flower fabricated electrochemical sensor, *Sensors Actuators, B Chem.* 192 (2014) 1–8.
- [26] X. Xia, Z. Zheng, Y. Zhang, X. Zhao, C. Wang, Synthesis of Ag-MoS<sub>2</sub>/chitosan nanocomposite and its application for catalytic oxidation of tryptophan, *Sensors Actuators, B Chem.* 192 (2014) 42–50.
- [27] K.J. Huang, Y.J. Liu, Y.M. Liu, L.L. Wang, Molybdenum disulfide nanoflower-chitosan-au nanoparticles composites based electrochemical sensing platform for bisphenol a determination, *J. Hazard. Mater.* 276 (2014) 207–215.
- [28] M. Wang, Y. Shi, Y. Zhang, Y. Wang, H. Huang, J. Zhang, J. Song, Sensitive Electrochemical Detection of Bisphenol A Using Molybdenum Disulfide/Au Nanorod Composites Modified Glassy Carbon Electrode, *Electroanalysis.* (2017) 1–9.
- [29] S. Su, H. Sun, F. Xu, L. Yuwen, C. Fan, L. Wang, Direct electrochemistry of glucose oxidase and a biosensor for glucose based on a glass carbon electrode modified with MoS<sub>2</sub> nanosheets decorated with gold nanoparticles, *Microchim. Acta.* 181 (2014) 1497–1503.
- [30] O. Parlak, A. Incel, L. Uzun, A.P.F. Turner, A. Tiwari, Structuring Au nanoparticles on two-dimensional MoS<sub>2</sub> nanosheets for electrochemical glucose biosensors, *Biosens. Bioelectron.* 89 (2017) 545–550.
- [31] T. Wang, H. Zhu, J. Zhuo, Z. Zhu, P. Papakonstantinou, G. Lubarsky, J. Lin, M. Li, Biosensor Based on Ultrasmall MoS<sub>2</sub> Nanoparticles for Electrochemical Detection of H<sub>2</sub>O<sub>2</sub> Released by Cells at the Nanomolar Level, *Anal. Chem.* 85 (2013) 10289–10295.
- [32] I. Vasilescu, S.A.V. Eremia, M. Kusko, A. Radoi, E. Vasile, G.L. Radu, Molybdenum disulphide and graphene quantum dots as electrode modifiers for laccase biosensor, *Biosens. Bioelectron.* 75 (2016) 232–237.
- [33] H. Song, Y. Ni, S. Kokot, Investigations of an electrochemical platform based on the layered MoS<sub>2</sub>-graphene and horseradish peroxidase nanocomposite for direct electrochemistry and electrocatalysis, *Biosens. Bioelectron.* 56 (2014) 137–143.
- [34] M.Z.M. Nasir, C.C. Mayorga-Martinez, Z. Sofer, M. Pumera, Two-Dimensional 1T-Phase Transition Metal Dichalcogenides as Nanocarriers to Enhance and Stabilize Enzyme Activity for Electrochemical Pesticide Detection, *ACS Nano.*

- 11 (2017) 5774–5784.
- [35] A.M. Parra-Alfambra, E. Casero, M.D. Petit-Domínguez, M. Barbadillo, F. Pariente, L. Vázquez, E. Lorenzo, New nanostructured electrochemical biosensors based on three-dimensional (3-mercaptopropyl)-trimethoxysilane network, *Analyst*. 136 (2011) 340–347.
- [36] O.A. Loaiza, P.J. Lamas-Ardisana, L. Añorga, E. Jubete, V. Ruiz, M. Borghei, G. Caballero, H.J. Grande, Graphitized carbon nanofiber-Pt nanoparticle hybrids as sensitive tool for preparation of screen printing biosensors. Detection of lactate in wines and ciders, *Bioelectrochemistry*. 101 (2015) 58–65.
- [37] Y. Zhao, X. Fang, Y. Gu, X. Yan, Z. Kang, X. Zheng, P. Lin, L. Zhao, Y. Zhang, Gold nanoparticles coated zinc oxide nanorods as the matrix for enhanced l-lactate sensing, *Colloids Surfaces B Biointerfaces*. 126 (2015) 476–480.
- [38] M. Briones, E. Casero, M.D. Petit-Domínguez, M.A. Ruiz, A.M. Parra-Alfambra, F. Pariente, E. Lorenzo, L. Vazquez, Diamond nanoparticles based biosensors for efficient glucose and lactate determination, *Biosens. Bioelectron*. 68 (2015) 521–528.
- [39] M. Briones, M.D. Petit-Domínguez, A.M. Parra-Alfambra, L. Vázquez, F. Pariente, E. Lorenzo, E. Casero, Electrocatalytic processes promoted by diamond nanoparticles in enzymatic biosensing devices, *Bioelectrochemistry*. 111 (2016) 93–99.
- [40] M. Briones, E. Casero, L. Vazquez, F. Pariente, E. Lorenzo, M.D. Petit-Domínguez, Diamond nanoparticles as a way to improve electron transfer in sol-gel l-lactate biosensing platforms, *Anal. Chim. Acta*. 908 (2016).
- [41] E. Casero, C. Alonso, L. Vázquez, M.D. Petit-Domínguez, A.M. Parra-Alfambra, M. de la Fuente, P. Merino, S. Álvarez-García, A. de Andrés, F. Pariente, E. Lorenzo, Comparative Response of Biosensing Platforms Based on Synthesized Graphene Oxide and Electrochemically Reduced Graphene, *Electroanalysis*. 25 (2013) 154–165.
- [42] H. Teymourian, A. Salimi, S. Khezrian, Fe<sub>3</sub>O<sub>4</sub> magnetic nanoparticles/reduced graphene oxide nanosheets as a novel electrochemical and bioelectrochemical sensing platform, *Biosens. Bioelectron*. 49 (2013) 1–8.
- [43] E. Casero, C. Alonso, M.D. Petit-Domínguez, L. Vazquez, A.M. Parra-Alfambra, P. Merino, S. Alvarez-Garcia, A. de Andres, E. Suarez, F. Pariente, E. Lorenzo, Lactate biosensor based on a bionanocomposite composed of titanium oxide nanoparticles, photocatalytically reduced graphene, and lactate oxidase, *Microchim. Acta*. 181 (2014) 79–87.
- [44] S. Azzouzi, L. Rotariu, A.M. Benito, W.K. Maser, M. Ben Ali, C. Bala, A novel amperometric biosensor based on gold nanoparticles anchored on reduced graphene oxide for sensitive detection of l-lactate tumor biomarker, *Biosens. Bioelectron*. 69 (2015) 280–286.
- [45] B. Manna, C. Retna Raj, Covalent functionalization and electrochemical tuning of reduced graphene oxide for the bioelectrocatalytic sensing of serum lactate, *J. Mater. Chem. B*. 4 (2016) 4585–4593.
- [46] J.M. Goran, J.L. Lyon, K.J. Stevenson, Amperometric detection of l-lactate using nitrogen-doped carbon nanotubes modified with lactate oxidase, *Anal. Chem*. 83 (2011) 8123–8129.
- [47] A.C. Çelik, F. Öztürk, P.E. Erden, C. Kaçar, E. Kılıç, Amperometric Lactate Biosensor Based on Carbon Paste Electrode Modified with Benzo[ c ]cinnoline and Multiwalled Carbon Nanotubes, *Electroanalysis*. 27 (2015) 2820–2828.
- [48] N. Hernández-Ibáñez, L. García-Cruz, V. Montiel, C.W. Foster, C.E. Banks, J.

- Iniesta, Electrochemical lactate biosensor based upon chitosan/carbon nanotubes modified screen-printed graphite electrodes for the determination of lactate in embryonic cell cultures, *Biosens. Bioelectron.* 77 (2016) 1168–1174.
- [49] G. Cunningham, M. Lotya, C.S. Cucinotta, S. Sanvito, S.D. Bergin, R. Menzel, M.S.P. Shaffer, J.N. Coleman, Solvent Exfoliation of Transition Metal Dichalcogenides : Dispersability of Exfoliated Nanosheets Varies Only Weakly Between Compounds Solvent Exfoliation of Transition Metal Dichalcogenides : Dispersability of Exfoliated Nanosheets Varies Only Weakly Bet, *ACS Nano.* 6 (2012) 3468–3480.
- [50] J.N. Coleman, M. Lotya, A. O'Neill, S.D. Bergin, P.J. King, U. Khan, K. Young, A. Gaucher, S. De, R.J. Smith, I. V. Shvets, S.K. Arora, G. Stanton, H.-Y. Kim, K. Lee, G.T. Kim, G.S. Duesberg, T. Hallam, J.J. Boland, J.J. Wang, J.F. Donegan, J.C. Grunlan, G. Moriarty, A. Shmeliov, R.J. Nicholls, J.M. Perkins, E.M. Grieveson, K. Theuwissen, D.W. McComb, P.D. Nellist, V. Nicolosi, Two-Dimensional Nanosheets Produced by Liquid Exfoliation of Layered Materials, *Science.* 331 (2011) 568–571.
- [51] R.J. Smith, P.J. King, M. Lotya, C. Wirtz, U. Khan, S. De, A. O'Neill, G.S. Duesberg, J.C. Grunlan, G. Moriarty, J. Chen, J. Wang, A.I. Minett, V. Nicolosi, J.N. Coleman, Large-scale exfoliation of inorganic layered compounds in aqueous surfactant solutions, *Adv. Mater.* 23 (2011) 3944–3948.
- [52] H. Vallhov, S. Gabrielsson, M. Strømme, A. Scheynius, A.E. Garcia-Bennett, Mesoporous silica particles induce size dependent effects on human dendritic cells, *Nano Lett.* 7 (2007) 3576-3582.
- [53] Y. Wang, T. Li, W. Zhang, Y. Huang, A hydrogen peroxide biosensor with high stability based on gelatin-multiwalled carbon nanotubes modified glassy carbon electrode, *J. Solid State Electrochem.* 18 (2014) 1981-1987.
- [54] Z. Matharu, P. Pandey, M.K. Pandey, V. Gupta, B.D. Malhotra, Functionalized gold nanoparticles-octadecylamine hybrid Langmuir-Blodgett film for enzyme sensor, *Electroanalysis* 21 (2009) 1587-1596.
- [55] X. Ren, F. Tang, R. Liao, L. Zhang, Using gold nanorods to enhance the current response of a choline biosensor, *Electrochimica Acta* 54 (2009) 7248-7253.

## CAPTION OF FIGURES

### Scheme 1. Lactate detection principle.

**Figure 1.** CV response of GC electrodes modified with MoS<sub>2</sub>/LOx in contact with 0.1 M pH = 7 phosphate buffer containing 1 mM of HMF in the absence (a), and presence of 0.65 mM L-lactate where MoS<sub>2</sub>, of 90 nm particle size, has been exfoliated in IPA/water (b), EtOH/water (c), DMF (d) and NMP (e). Scan rate: 10 mV s<sup>-1</sup>.

**Figure 2.** CV response of GC electrodes modified with MoS<sub>2</sub> (exfoliated in NMP) and LOx in contact with 0.1 M pH = 7 phosphate buffer containing 1 mM of HMF in the absence (a), and presence of 0.65 mM L-lactate where MoS<sub>2</sub> has a particle size of 2 μm (b) and 90 nm (c). Scan rate: 10 mV s<sup>-1</sup>.

**Figure 3.** Intensities of the anodic peak current obtained from cyclic voltammetric measurements at +0.30 V for GC electrodes modified with different concentrations of 90 nm MoS<sub>2</sub> in NMP. [HMF] = 1 mM in 0.1 M pH = 7 phosphate buffer. [L-lactate] = 0.25 mM. Other conditions: scan rate: 10 mV s<sup>-1</sup>.

**Figure 4.** (a) 10 x 10 μm<sup>2</sup> AFM image of a sample prepared by depositing a drop of NMP on silicon and let it to dry. (b) 2.5 x 2.5 μm<sup>2</sup> topographical AFM image of a sample containing MoS<sub>2</sub> exfoliated in NMP. (c) Surface profile corresponding to the solid line in (b). Topographical (d) and KFM (e) 2 x 2 μm<sup>2</sup> images taken simultaneously on an area displaying a flake. The vertical scale in the KFM image corresponds to the CPD signal. Note the different contrast in the KFM image at the flake. (f) 480 x 360 nm<sup>2</sup> AFM image of a sample with MoS<sub>2</sub> exfoliated in NMP and with LOx. (g) Surface profile along the line depicted in (f). (h) 360 x 360 nm<sup>2</sup> AFM taken in other location of the sample imaged in (f).

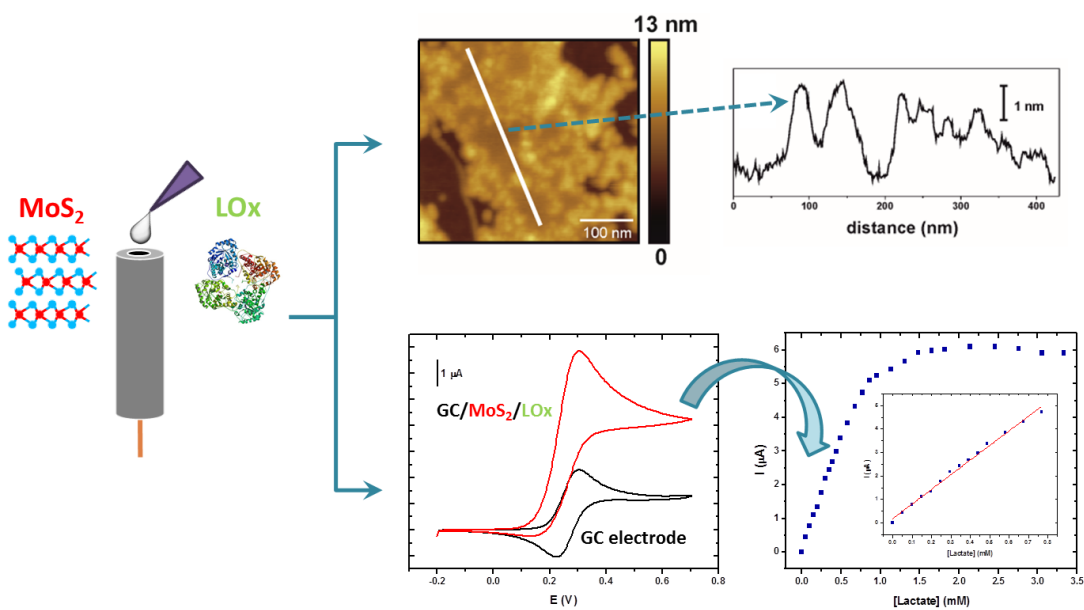
**Figure 5.** Electrochemical impedance spectra obtained in a 0.1 M phosphate buffer (pH = 7), containing 10 mM [Fe(CN)<sub>6</sub>]<sup>3-/4-</sup> for: (a) GC bare, (b) GC/LOx, (c) GC/MoS<sub>2</sub>/LOx and (d) GC/MoS<sub>2</sub> systems. The inset corresponds to an amplification of curve a.

**Figure 6. A.** Cyclic voltammograms obtained for 1 mM HMF in presence of different concentrations of lactate (expressed in mM): (a) 0.050, (b) 0.149, (c) 0.247, (d) 0.344, (e) 0.440, (f) 0.582, (g) 0.676 and (h) 0.769. Scan rate: 10 mV s<sup>-1</sup>. **B.** Calibration curve obtained from current intensity measured at +0.30 V. The inset shows the linear concentration range.

MoS<sub>2</sub> nanosheets for improving analytical performance of lactate biosensors

Ana María Parra-Alfambra, Elena Casero, Luis Vázquez, Carmen Quintana, María del Pozo,  
María Dolores Petit-Domínguez

GRAPHICAL ABSTRACT



## **HIGHLIGHTS**

- ✓ Integration of MoS<sub>2</sub> nanosheets and lactate oxidase enzyme in 2D biosensors
- ✓ MoS<sub>2</sub> nanosheets are obtained by a liquid exfoliation method
- ✓ Biosensors containing both components exhibit the best electrocatalytic response

SCHEME 1

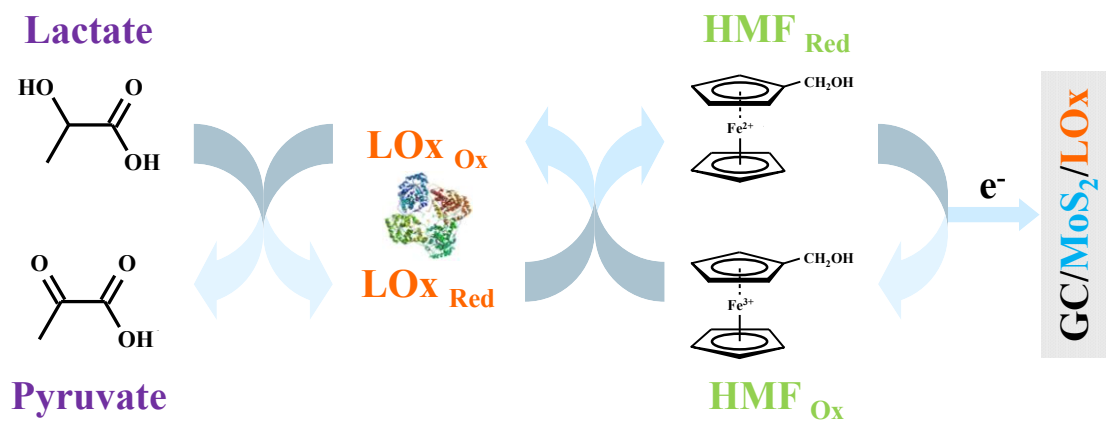




Figure 1

FIGURE 1

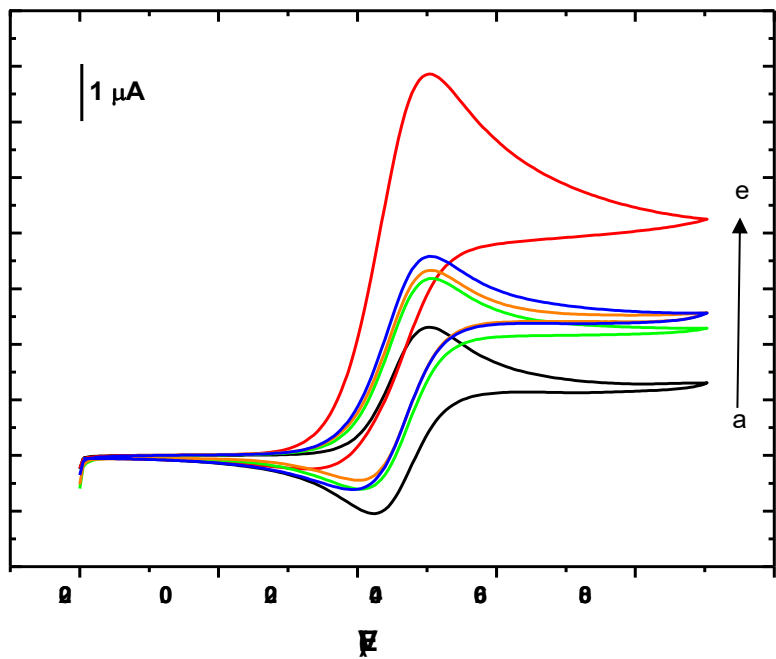


Figure 2

FIGURE 2

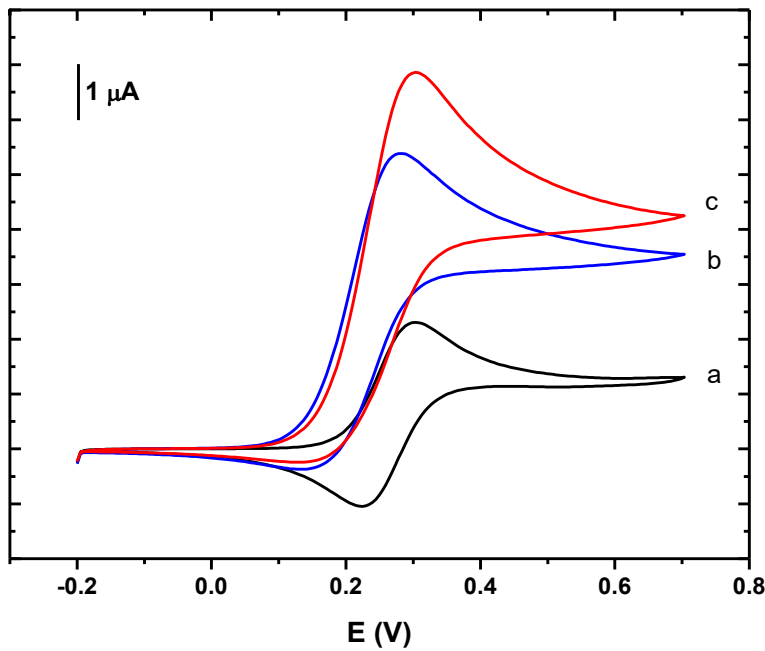


Figure 3

FIGURE 3

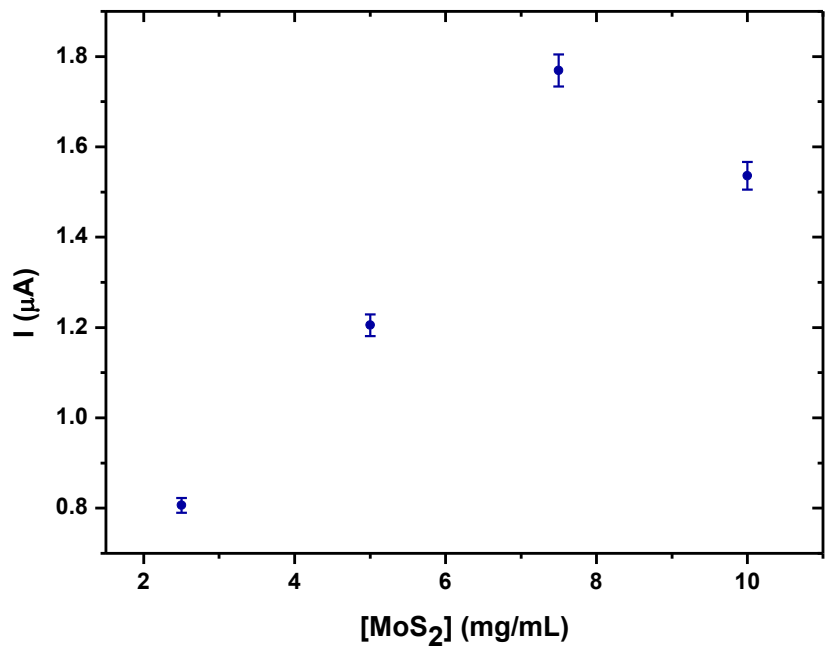


Figure 4

FIGURE 4

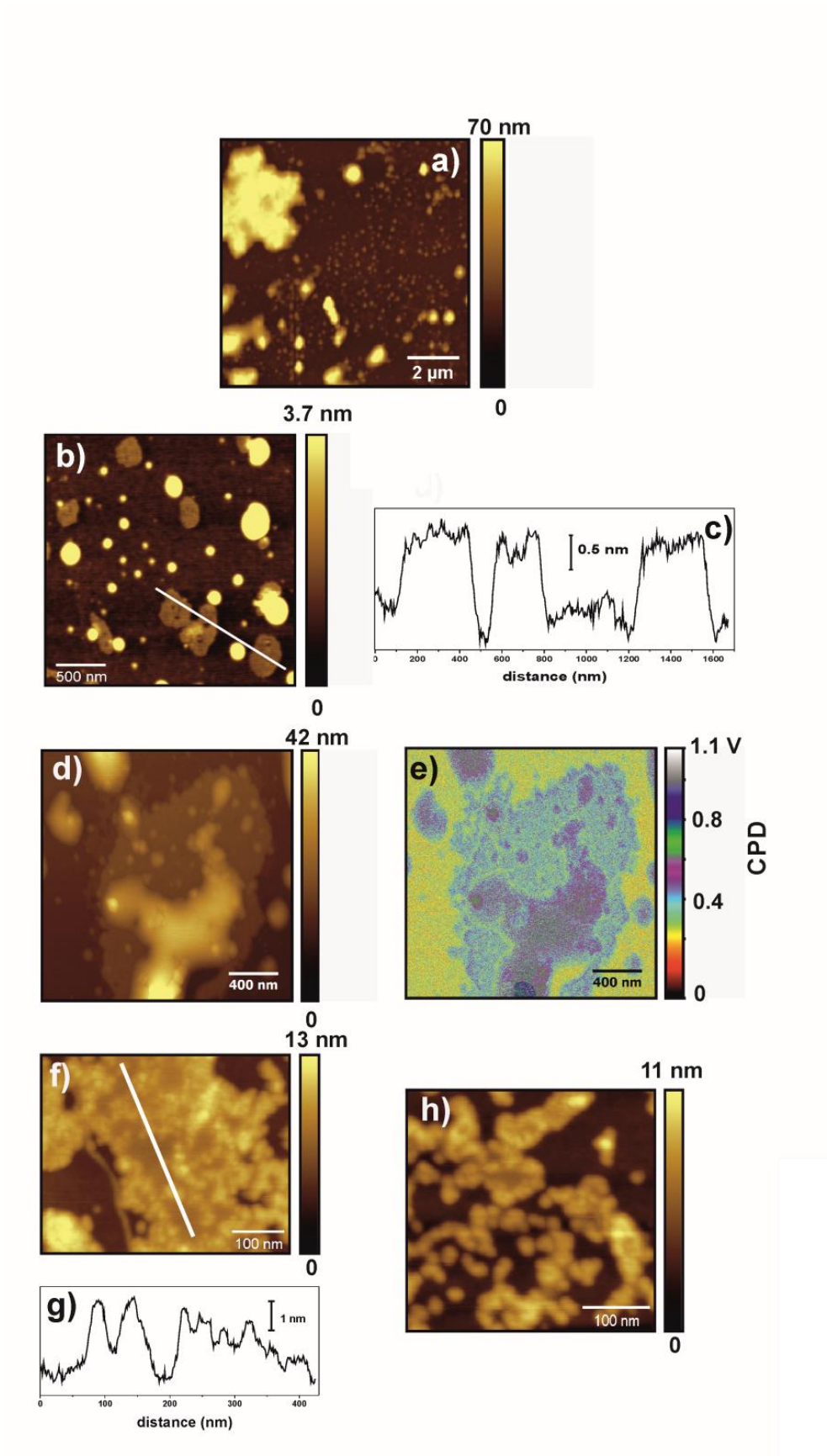


Figure 5

FIGURE 5

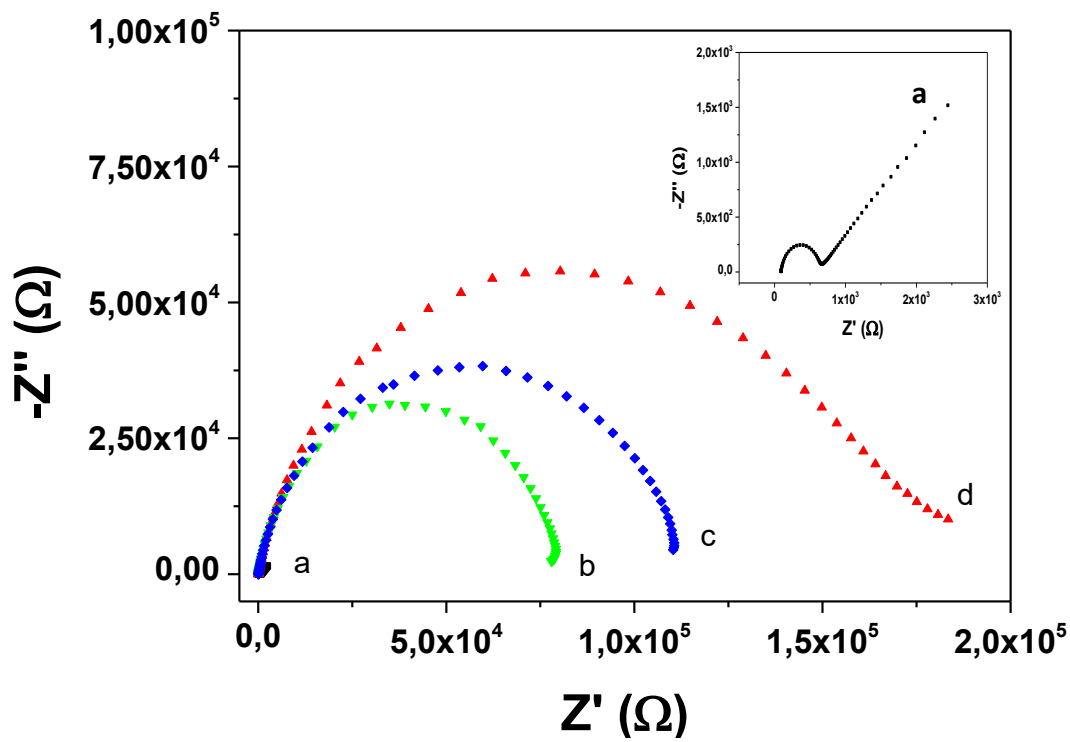


Figure 6

FIGURE 6

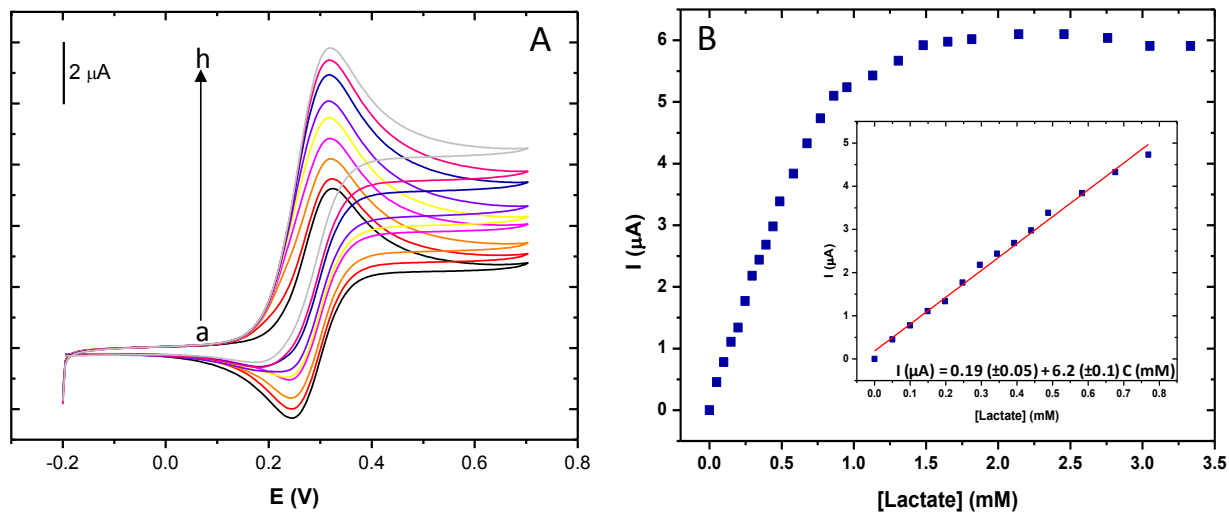


Table 1

REFERENCE	ELECTRODE MODIFICATION	LINEAR CONCENTRATION RANGE (mM)	SENSITIVITY ( $\mu\text{AmM}^{-1}$ )	DETECTION LIMIT ( $\mu\text{M}$ )	R.S.D. (%)
Present work	GC/MoS <sub>2</sub> /LOx	0.056 - 0.77	6.22	17	1.7 (n=10)
[35]	Au/MPTS/AuNPs/LOx	0.05 -0.25	3.4	4.0	2 (n=10)
[36]	LOx/PtNPs/GCNF/SPCEs	0.01 - 2.0	0.0413 *	6.9	1.8 (n=10)
[37]	LOx/AuNPs/ZnO NRs/Au	0.01 - 0.6	24.56 *	6	4.23 (n=5)
[38]	Au /DNPs9/ LOx	0.05 -0.7	4.0	15	5 (n=9)
[39]	Au/ DNPs4/LOx	0.02 -1.2	6.1	5.3	1 (n=50)
[40]	Au/MPTS/DNPs9/LOx	0.053 -1.6	2.6	16	7.0 (n=3)
[41]	GC/GO/LOx	0.018 -0.58	6.5	5.5	3.0 (n=5)
[41]	GC/ERG/LOx	0.025 -0.25	3.2	7.5	6.1 (n=5)
[42]	LDH/Fe <sub>3</sub> O <sub>4</sub> /r-GO/GC	0.2 -2.2	22.6 *	20	-----
[43]	GC/PRG/TiO <sub>2</sub> /LOx	0.002 -0.40	6.0	0.60	3.2 (n=5)
[44]	LDH/ r-GO/AuNPs/SPCEs	0.01 –5	154 *	0.13	1.57 (n=20)
[45]	LDH/ rGO- PhNHOH/GC	Up to 0.090	10.57 *	2.5	-----
[46]	LOx/N-CNTs/GC	0.014 -0.325	40 *	4.1	1.6 (n=10)
[47]	LOx/BCC/MWCNTs/CPE	0.0002 -0.11	-----	0.07	2.5 (n=7)
[48]	MWCNTs/CS/LOx/SPBGE	0.03 -0.24	3.417	22.6	5 (n=7)

Table 1. Analytical properties of lactate biosensors found in the literature  
Glassy carbon (GC); Molybdenum disulfide (MoS<sub>2</sub>); Lactate oxidase (LOx); (3-mercaptopropyl)-trimethoxysilane (MPTS); gold nanoparticles (AuNPs); platinum nanoparticles (PtNPs); graphitized carbon nanofibers (GCNF); screen printed carbon electrodes (SPCEs); zinc oxide nanorods (ZnO NRs); diamond nanoparticles of 9 nm (DNPs9); diamond nanoparticles of 4 nm (DNPs4); graphene oxide (GO); electrochemically reduced graphene (ERG); Lactate dehydrogenase (LDH); Fe<sub>3</sub>O<sub>4</sub> magnetic nanoparticles (Fe<sub>3</sub>O<sub>4</sub>); reduced graphene oxide (r-GO); photocatalytically reduced graphene (PRG); TiO<sub>2</sub> nanoparticles (TiO<sub>2</sub>); derivatized reduced graphene oxide (r-GO-PhNHOH); Nitrogen-doped carbon nanotubes (N-CNTs); Benzo[c]cinnoline (BCC); multiwalled carbon nanotubes (MWCNTs); carbon paste electrode (CPE); chitosan (CS); basal-plane like screen-printed graphite electrodes (SPBGEs); \*sensitivity value normalized by cm<sup>2</sup>

Table 2. Interferences study ([lactate] = 0.25 mM).

Potential Interferent	Ratio [Interferent]/[Lactate]	$\Delta I$ (%)
Dopamine	0.25	12
Ascorbic acid	0.53	11
Uric acid	1.0	13
Citric acid	3.0	11



## Biographies

**Ana María Parra-Alfambra** received her degree in Analytical Chemistry and her PhD degree from Universidad Autónoma de Madrid in 2000 and 2008, respectively. Since 2013 she is Associate Professor in the Department of Analytical Chemistry and Instrumental Analysis at the Universidad Autónoma de Madrid. Her current research interests consist of the incorporation of different nanomaterials in the development of electrochemical biosensors.

**Elena Casero Junquera** is Professor in the Department of Analytical Chemistry and Instrumental Analysis at the Universidad Autónoma de Madrid. She received her degree in Chemistry in 1991 from the Universidad Complutense de Madrid and her PhD degree in 1996 from the Université de Paris-Sud. Afterwards, she was a CAM postdoctoral fellow at Universidad Autónoma de Madrid from 1997–1998. From 1999 to 2010, she was Associate Professor at the Universidad Autónoma de Madrid. Her current research is focused on the development, characterization and application of bioanalytical platforms based on different nanomaterials, such as gold nanoparticles, carbon nanotubes, graphene and diamond nanoparticles.

**Luis Vázquez Burgos** is Full Professor of the Spanish National Research Council (CSIC). He made his PhD. in Physics in 1989. Afterwards, he made a post-doctoral stage at ESRF (Grenoble, France). He belongs to the scientific staff of the Instituto de Ciencia de Materiales de Madrid since 1990. He has published more than 220 papers in international scientific journals and several book chapters. His research interests are the study of growing/etching interfaces, surface nano-patterning and AFM, in particular applied to the study of biomolecules and biointerfaces.

**Carmen Quintana** received her degree in Chemistry in 1991 from the Universidad Autónoma de Madrid and her PhD degree in 1998 from the same University. Since 2010 she is Professor at the Department of Analytical Chemistry and Instrumental Analysis at the Universidad Autónoma de Madrid. Her current research is focused on the development and characterization of electrochemical sensors based on macrocyclic receptors and different nanomaterials (i.e. gold nanoparticles or graphene among others).

**Maria del Pozo** received her degree and PhD degree in Chemistry from the Universidad Autónoma de Madrid (Spain) in 2008 and 2013, respectively. Afterwards,

she was a CONICET postdoctoral fellow at INQUIMAE (Buenos Aires, Argentina) from 2014-2016. Her areas of interests include the development and application of (electro)chemical sensors based on macrocyclic receptors and different nanomaterials. Since 2017, she is Assistant Professor at the Department of Analytical Chemistry and Instrumental Analysis at Universidad Autónoma de Madrid.

**Maria Dolores Petit-Dominguez** received her degree and her PhD degree in Chemistry from the Universidad Autónoma de Madrid in 1987 and 1992, respectively. Afterwards, she made a post-doctoral stage at the Department of Chemistry at University of Cincinnati (Ohio, USA), where she began her research in the development of electrochemical sol-gel sensors. Since 1992 she is Professor of Analytical Chemistry in the Department of Analytical Chemistry and Instrumental Analysis at the Universidad Autónoma de Madrid and her current research is focused on the development and characterization of chemical (bio)sensors based on nanomaterials.